Monitoring DBP formation with differential UV spectroscopy

A new application uses differential UV spectroscopy to monitor DBP formation easily, rapidly, and inexpensively.

Chi-Wang Li, Gregory V. Korshin, and Mark M. Benjamin

The decrease in the ultraviolet (UV) absorbance of natural organic matter (NOM) induced by chlorination can be characterized by the differential UV spectrum of the water. Differential UV spectra of chlorinated NOM are remarkably similar for a wide range of water qualities and chlorination conditions, always exhibiting a band with a maximum near a wavelength of 272 nm. The magnitude of the decrease in A_{272} (ΔA_{272}) is an excellent indicator of total organic halogen (TOX) formation resulting from chlorination, independent of the ratio of chlorine to dissolved organic carbon, bromide concentration, pH, reaction time, and NOM source. Use of ΔA_{272} as a surrogate allows virtually instantaneous and continuous monitoring of TOX and in some cases, specific disinfection by-products, at a much lower cost than is possible using conventional analytical approaches.

Reactions of natural organic matter (NOM) with halogen-containing disinfectants generate unwanted disinfection by-products (DBPs). Such DBPs can be quantified as individual species (e.g., chloroform [$CHCl_3$]) or groups of species (e.g., trihalomethanes [THMs] and haloacetic acids [HAAs]) or by the total organic halogen (TOX) concentration, a composite parameter characterizing the incorporation of halogen into all organic molecules regardless of their identity. Currently only about 50 percent of the TOX can be assigned to individual species.[1–4] The toxicological signifi-

For executive summary, see page 174.

The natural organic matter used in most of the experiments as concentrated from Judy Reservoir—a low-hardness, low-total-dissolved-solids source that supplies Mt. Vernon, Wash.

cance of TOX cannot be established in the absence of detailed information about the specific compounds that contribute to it. Nonetheless this parameter does provide a measure of the overall DBP formation that cannot be provided by analyses of specific DBPs.

The relationships among chlorination conditions—pH, temperature, reaction time, bromide concentration, chlorine dosage, and NOM concentration; NOM characteristics—hydrophobicity, functional group content, specific ultraviolet absorbance (SUVA, i.e., UV absorbance per milligram per litre dissolved organic carbon [DOC]); and the formation of DBPs are highly nonlinear and complex.[5–8] Attempts to develop formal kinetic or statistical models for DBP formation have been impeded by the substantial cost and effort of analyzing for DBPs. These impediments restrict the amount of data that can be obtained in any laboratory or field study of the chlorination reaction and thereby limit the information available to formulate or test models of the reaction sequence.

This article describes a method that virtually eliminates these limitations on TOX analysis and perhaps on analysis of certain individual DBPs as well. The method is based on changes in the UV absorbance spectrum of NOM-containing solutions when they are chlorinated. Changes in the spectrum of NOM that are induced by removal or alteration of specific light-absorbing groups (chromophores) also provide insight into the reactivity and structure of NOM molecules. The first part of the article reviews the fundamentals of UV absorbance and ways in which UV spectra of natural water can be analyzed. The second part describes an approach for using spectral data to understand and quantify DBP formation.

Background

UV absorbance spectrum of NOM. The UV absorbance spectra of pure compounds dissolved in water consist of absorbance bands with well-defined maximum values at wavelengths that correspond to the energy needed to promote an electron in the molecule to a higher energy orbital. Most aromatic compounds have three such bands.[9,10]

The absorbance of light by a natural water sample is an additive property of all the chromophores in the sample. Although a variety of functional groups can contribute to the absorbance of a natural water sample, the strong correlation between UV absorbance and the aromatic carbon content of the sample[11,12] suggests that most of the absorbance of natural water at $\lambda > 250$ nm is caused by aromatic groups. The broad diversity of the chromophores in NOM molecules causes the different absorbance bands to overlap and merge so that the overall UV absorbance spectrum of a natural water resembles a single, smooth hump. The absence of distinct peaks in the spectrum has dissuaded researchers from analyzing it in detail, with the result that the use of UV spectroscopy to study NOM has consisted almost entirely of reports of the UV absorbance at a single, characteristic wavelength (λ), typically 254 nm, or SUVA at the same wavelength ($SUVA_{254}$).

Differential UV spectroscopy focuses not on the overall UV spectrum of the water but on the change in UV absorbance induced by the chlorination reaction.

Korshin et al[13] reported that despite its relatively featureless appearance, the UV spectrum of NOM can be represented very accurately as a composite of three distinct bands, each of which might include contributions from many different chromophores in the NOM. Each band was characterized mathematically by representing the absorbance as a Gaussian function of the energy of the absorbed light. When the UV spectra of NOM from several sources were analyzed using this model, the parameters defining the various Gaussian

TABLE 1 Treatment sequence at utilities 1–5

Treatment Sequence	Utility 1	Utility 2	Utility 3	Utility 4	Utility 5
pH adjustment		✓ (CO_2)			✓ (CO_2)
Prechlorination	✓ (ClO_2)		✓ (Cl_2)	✓ (ClO_2)*	
Coagulation	✓	✓ ($FeCl_3$)	✓ ($FeCl_3$)	✓ (Alum or powdered activated carbon)	✓ (Alum + $FeCl_3$)
Powdered activated carbon			✓		
Settling	✓	✓	✓	✓	✓
Softening			✓		
Ozonation	✓		✓		
Other				ClO_2 or Cl_2*	ClO_2 or Cl_2*
Softening			✓		
Sand filtration	✓	✓	✓	✓	✓
Ozonation		✓	✓	✓	✓
Granular activated carbon		✓		✓	

*Added intermittently

curves were similar in all the samples, supporting the basic premise of the model. The authors believed that the values of those parameters might provide insight into NOM structure and reactivity. For instance, the values suggested that the intensity and width of one of the bands (the electron-transfer or ET band, which peaks in the range 250–255 nm) might be related to the concentration and type of aromatic chromophores in the NOM.

Differential UV spectroscopy. Because aromatic functional groups are thought to be both the dominant chromophores in NOM and the dominant sites of attack by chlorine (Cl) on NOM molecules, the absorbance at 254 nm (A_{254}) has frequently been proposed as an indicator of the concentration of DBP precursor sites in a water sample.[14,15] However, the success of models that rely on A_{254} to predict DBP formation under typical chlorination conditions in water treatment systems has been marginal at best.

Although the use of UV spectroscopy to predict DBP formation is problematic, preliminary reports[13,16] have shown that a technique known as differential UV spectroscopy can be an extremely effective tool for monitoring the amount of DBPs formed by chlorination. Differential UV spectroscopy focuses not on the overall UV spectrum of the water but on the change in UV absorbance induced by the chlorination reaction. Specifically, the differential UV spectrum of chlorinated NOM is defined as

$$\Delta A_\lambda = A_\lambda^{init} - A_\lambda^{chl} \qquad (1)$$

in which A_λ^{init} is the absorbance of light at wavelength λ prior to chlorination, A_λ^{chl} is the absorbance of light at wavelength λ after chlorination, and ΔA_λ is the differential absorbance at wavelength λ.

The differential spectrum detects both the chromophores that are destroyed by the reaction and any that are generated. In contrast, any nonreacting chromophores in the sample contribute the same absorbance to the original and chlorinated samples and therefore do not appear in the differential spectrum. Thus, by its nature, differential spectroscopy focuses strictly on the light-absorbing sites that are involved in the reaction. This feature of differential spectroscopy is very attractive because it expands differential spectroscopy's applicability to water qualities in which the performance of conventional UV spectroscopy may be compromised by interfering species. If, as several authors have suggested, the reaction of chlorine with NOM takes place primarily at sites that absorb UV light, differential UV spectroscopy could provide a sensitive and highly targeted probe into the chlorination reaction.

Korshin et al[16] reported that ΔA_{272} is linearly correlated with the generation of TOX in a chlorinated sample, as shown by Eq 2:

$$\text{TOX generated} = k\,\Delta A_{272} \qquad (2)$$

They also reported that a single regression line could describe the TOX versus ΔA_{272} relationship in a variety of natural water samples chlorinated under a wide range of conditions (e.g., pH, NOM concentration, Cl dosage, reaction time). The best-fit value

TABLE 2 Analytical data for raw and treated water at utilities 1–5*

Utility	DOC† *mg/L*	A_{254} *cm^{-1}*	$SUVA_{254}$ *L/mg-m*	Br *µg/L*
Raw Water				
1	6.13 ± 0.57	0.231 ± 0.033	3.8 ± 0.3	<25
2	5.84 ± 0.70	0.181 ± 0.026	2.7 ± 0.2	74 ± 19
3	10.06 ± 1.76	0.262 ± 0.036	2.8 ± 0.3	187 ± 61
4	8.04 ± 1.44	0.343 ± 0.063	4.5 ± 0.2	75 ± 15
5	9.95 ± 2.65	0.308 ± 0.091	3.2 ± 0.2	215 ± 77
Treated Water				
1	2.18 ± 0.36	0.027 ± 0.006	1.5 ± 0.7	<25
2	1.70 ± 0.39	0.019 ± 0.006	1.1 ± 0.2	84 ± 17
3	2.74 ± 0.39	0.025 ± 0.006	0.9 ± 0.2	67 ± 25
4	1.58 ± 0.39	0.020 ± 0.008	1.3 ± 0.3	66 ± 15
5	3.40 ± 0.44	0.040 ± 0.010	1.2 ± 0.4	169 ± 78

*Samples analyzed monthly. Values are averages ± one standard deviation.
†A_{254}—absorbance at 254 nm, DOC—dissolved organic carbon, $SUVA_{254}$—specific ultraviolet absorbance at 254 nm

of k for the complete data set was 10,800 X µg TOX/L/cm^{-1} with an R^2 value of 0.99.

This result has two important implications. First, the fact that the best-fit regression line passes through the origin indicates that when Cl reacts with NOM, virtually all reactions that destroy UV absorbance are accompanied by incorporation of halogen into the organic molecule and vice versa. Second, the applicability of the relationship, regardless of the NOM source or concentration, the Cl dosage, the reaction time, and pH, suggests that the sites at which Cl incorporates into NOM molecules are the same in virtually all NOM–Cl reactions, independent of the source water quality or the chlorination conditions.

In a separate article, Korshin et al[13] reported a strong correlation between ΔA_{254} and generation of $CHCl_3$. However, the $CHCl_3$ versus ΔA_{254} correlation intersected the abscissa at $\Delta A_{254} > 0$, i.e., some UV absorbance was destroyed by the chlorination reaction before any $CHCl_3$ appeared in the water. Defining this amount of absorbance as ΔA^0_{254}, the relationship between $CHCl_3$ generation and ΔA_{254} can be represented by

$$CHCl_3 \text{ generated} = \begin{cases} 0 & \text{if } \Delta A_{254} < \Delta A^0_{254} \\ k' [\Delta A_{254} - \Delta A^0_{254}] & \text{if } \Delta A_{254} > \Delta A^0_{254} \end{cases} \quad (3)$$

The value of k' increased and that of ΔA^0_{254} decreased with increasing pH, consistent with the widespread observation that the yield of $CHCl_3$ in NOM chlorination reactions increases with pH.[17]

The relationship shown in Eq 3 reflects the fact that the generation of $CHCl_3$ is a multistep process. In the sequence leading to $CHCl_3$ formation, each reaction incorporating Cl into an NOM molecule destroys some UV absorbance and generates TOX (in accord with Eq 2), but $CHCl_3$ does not form until such reactions have proceeded to the point that they have destroyed an amount of absorbance equal to ΔA^0_{254} and formed an amount of TOX equal to $k\Delta A^0_{254}$.

In this research, the relationship between ΔA_λ and DBP generation was tested in systems containing bromide, expanded to consider formation of HAAs, and used to explore the kinetics and efficiency of Cl incorporation into NOM molecules.

FIGURE 1 Conventional (A) and differential (B) UV spectra for Judy Reservoir NOM chlorinated in the presence of 500 µg/ L Br^-

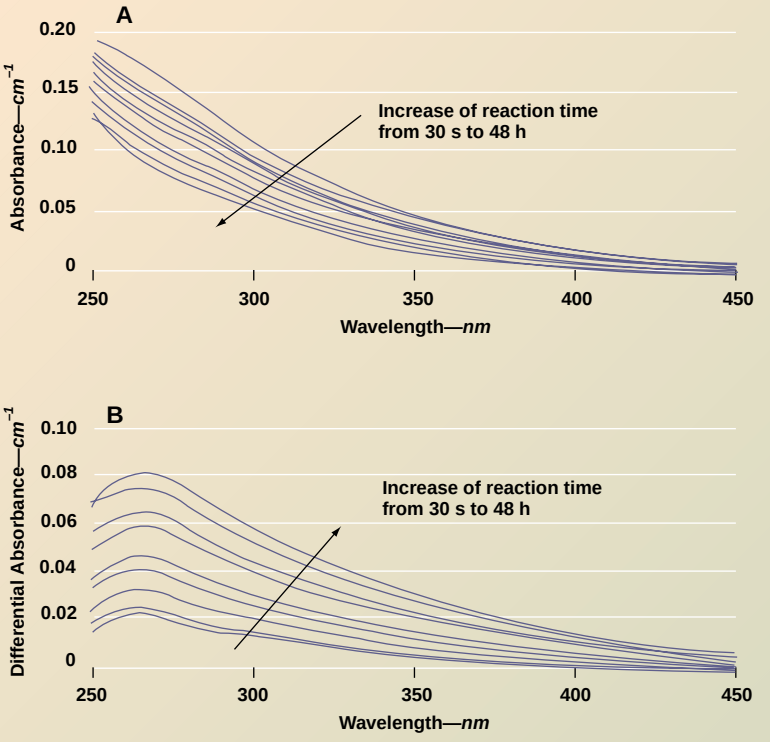

Methods and materials

All chemicals used in the study were of reagent quality. The NOM used in most of the experiments was concentrated from Judy Reservoir, the water supply for Mt. Vernon, Wash. This water source is low in hardness and total dissolved solids (TDS), with a pH of 7.0 ± 0.4 and a Br^- concentration below the study's detection limit of 25 µg/L. DOC concentrations and A_{254} values are typically in the ranges 3.0–4.5 mg/L and 0.11–0.16 cm^{-1}, respectively, yielding a typical $SUVA_{254}$ value of 3.3 L/mg-m. The NOM was concentrated by sorption onto iron oxide–coated sand[18] in packed columns, followed by elution with 0.5 M sodium hydroxide (NaOH). The eluent was immediately neutralized by passage through H^+-saturated cation exchange resin.* The eluent was then stored at 4°C until it was diluted with deionized water for use in experiments.

In the chlorination experiments, the pH of NOM-containing solutions was first adjusted to the desired value with NaOH or hydrochloric acid (HCl). Most experiments were run at pH 7.00 in the presence of phosphate buffer. The change of pH during the experiments was ≤0.35 units in all cases. In some experi-

*Biorad AG-MP-50, Hercules, Calif.

FIGURE 2 Differential UV spectra developed by titration of Judy Reservoir NOM with Cl

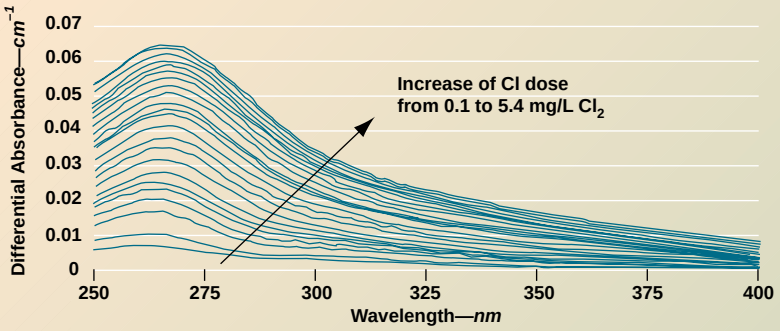

pH—7.0, DOC—5.2 mg/L, Cl dose—0.1 to 5.4 mg/L as Cl_2, reaction time—1 to 48 h

FIGURE 3 Normalized differential UV spectra for the titration of Judy Reservoir NOM titrated with Cl

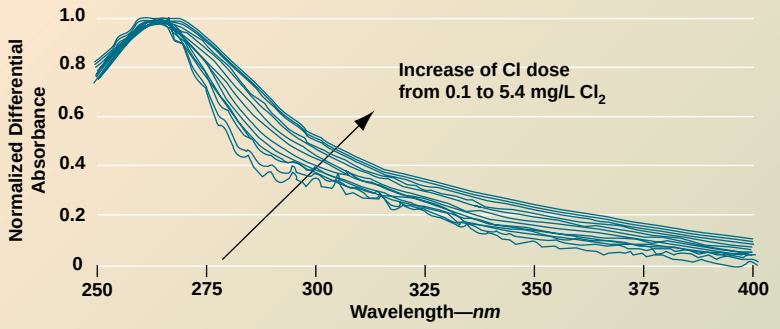

FIGURE 4 UV absorption spectra for raw and treated water from utility 4 before and after chlorination

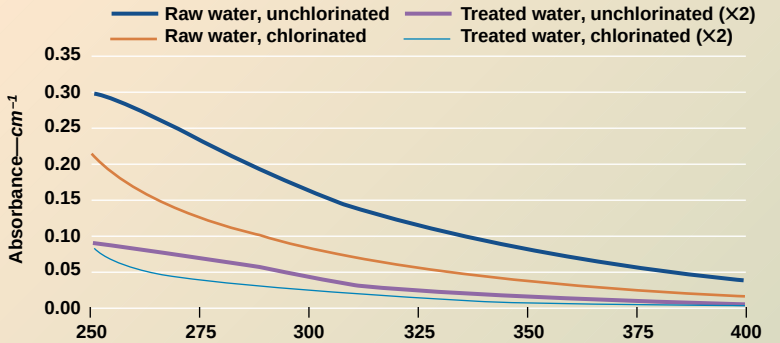

ments, potassium bromide was also added to the solutions prior to chlorination. Cl was added as sodium hypochlorite (NaOCl). Chlorinated samples were incubated at 20°C in headspace-free amber vials. Reaction times varied from a few seconds to 178 h, after which the reaction was usually stopped by addition of sodium sulfite (Na_2SO_3). However, in some experiments investigating chlorination at very low Cl-to-DOC ratios, all the Cl was consumed during the reaction period (confirmed by analysis of Cl residual), and no SO_3 was added.

DOC was measured using a carbon analyzer.* Prior to the analysis, samples were filtered through a prewashed polycarbonate 0.4-µm filter. UV spectra were recorded with a high-precision, high-dynamic-range dual-beam spectrophotometer† using matched 5-cm quartz cells. The precision of these measurements was critical for the analysis, because in many cases the change in the sample's absorbance upon chlorination was extremely small, especially in experiments studying short reaction times, low Cl dosages, or both. With the equipment used, the changes of UV absorbance could be reliably quantified for $\Delta A_{272} > 0.003$. This estimate of precision is three standard deviations (σ) calculated for a series of 24 measurements of absorbance for the raw water. The range of ΔA_{272} in the experiments discussed in this article typically far exceeded this 3σ threshold.

SO_3, which was used as a chlorine-quenching agent, has an absorbance peak centered at 195 nm that tails to approximately 250 nm. To eliminate interference from this species, differential spectra were analyzed only at wavelengths >250 nm. Other inorganic ions that might potentially interfere with analysis of UV absorbance (e.g., nitrate, nitrite, bromate, and chlorite) do not absorb strongly above 250 nm, were present at concentrations too low to cause significant interference, or both. Furthermore, nitrate—the ion in this group that has the greatest potential to cause significant interference—is not affected by chlorination. As a result, it does not contribute to the differential absorbance, even if it contributes significantly to the absorbance of the raw water.

The concentrations of bromide and other anions were determined using an ion chromatograph.‡ THM concentrations were determined by the pentane liquid–liquid extraction method (method 6232B)[19] using 10-mL samples and 2 mL of pentane. A gas chromatograph§ held at 260°C and equipped with an electron capture detector was used for these analyses. HAAs were analyzed according to US Environmental Protection Agency method 552.1.[20] TOX was analyzed by method 5320B[19] using a TOX analyzer.**

FIGURE 5 Differential spectra for raw and treated water from utility 4

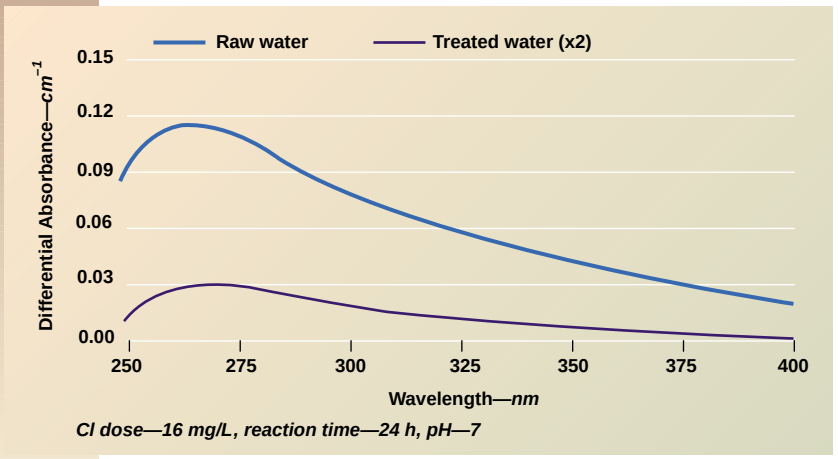

Samples of raw and treated water from five water treatment plants in France were also used in chlorination experiments. Samples were collected during the period February 1996 to February 1997 at plants operated by Societé d'Amenagement Urbain et Rurale (SAUR), and experiments and analyses were conducted in the SAUR laboratory in Maurepas, France. In the experiments, the five plants were designated utilities 1–5. Table 1 summarizes the treatment sequence used at these utilities. Table 2 summarizes some relevant water quality data for the raw and treated water.

In the experiments conducted in France, water samples (both raw and treated) were adjusted to pH 8.0 ± 0.2 with NaOH before they were dosed with sufficient NaOCl to provide 0.7–0.8 mg/L residual chlorine (as Cl_2) after a 24-h reaction period. After 24 h, the absorbance at 254 nm was measured with a spectrophotometer,†† using a 1-cm cell for raw water and a 5-cm cell for treated water samples. Because free Cl was not quenched prior to the UV measurements, the measured absorbance was corrected to subtract the contribution of free Cl. This correction was based on the measured concentration of free Cl in the sample and the specific absorbance of free Cl at 254 nm, which was determined independently. Concentrations of the four THMs formed in these water samples were determined using the standard French method AFNOR T 90-125.[21] A gas chromatograph coupled with a headspace injector‡‡ was used for THM analyses.

Sets of unchlorinated raw and treated water from the French treatment plants were sent to the University of Washington (Seattle) laboratory, where UV/visible spectra (200–800 nm) were recorded before and after chlorination. For these experiments, the pH of the samples was adjusted to 7.00 and buffered with phosphate before the samples were dosed with NaOCl (16 mg/L as Cl_2) and incubated at 20°C in 60-mL headspace-free amber vials for 24 h. Residual Cl was determined using the standard DPD–FAS titration method or its colorimetric version[19] and was quenched with Na_2SO_3 prior to analysis of the UV spectrum. The spectrophotometer and method for TOX analysis used were identical to those used for the experiments with Judy Reservoir water.

Results and discussion

Differential UV spectra of chlorinated NOM. Figure 1, part A shows a set of UV absorbance spectra for Judy Reservoir NOM subjected to chlorination; Figure 1, part B shows the corresponding differential spectra. For this experiment, a Cl dose of 17.6 mg/L as Cl_2 was applied to a solution containing 4.4 mg/L TOC, and the reaction was stopped by addition of Na_2SO_3 at times ranging from 30 s to 24 h after Cl addition. Although a clear trend of decreasing UV absorbance with increasing reaction time is apparent in part A of Figure 1, all of the absorbance spectra are broad curves that lack identifiable peaks. By contrast, part B of Figure 1 shows that the differential spectra calculated using Eq 1 have a well-defined peak near 270 nm that grows with increasing reaction time.

In the experiments characterized in Figure 1, a substantial amount of UV absorbance was destroyed within 30 s, i.e., before the first data were collected. In order to explore the early stages of the reaction between chlorine and NOM more thoroughly, a set of experiments was conducted in which small doses of Cl were added sequentially to a sample, starting with a Cl-to-DOC ratio of only 0.02 mg Cl_2/mg DOC. After each Cl addition, the system was allowed to react for 1 to 48 h, until all the free Cl had been consumed.

*OI 700, OI Corp., College Station, Texas
†Lambda-18, Perkin-Elmer, Norwalk, Conn.
‡DX-500 with AS-11 column and CD-20 conductivity detector, Dionex, Sunnyvale, Calif.
§AutoSystem GC with RTX-1 capillary column, Perkin-Elmer, Norwalk, Conn.
**TOX-10Σ, Mitsubishi, Tokyo, Japan
††Uvicon 930, Kontron Instruments, Milan, Italy
‡‡Varian 3400 chromatograph and Genesis headspace injector, Varian Corp., Palo Alto, Calif.

FIGURE 6 **Normalized average differential UV spectra for raw and treated water from utilities 1–5**

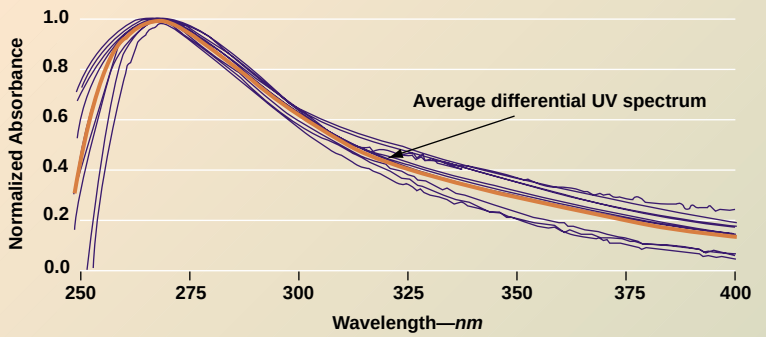

Each line represents the average spectrum of three water samples collected at different times at a given site. The bold line is the global average spectrum including all samples.

Presumably, in these experiments, the sites that were most reactive with Cl reacted with the initial Cl dosages, and progressively less reactive sites reacted as the dosage was increased.

Figure 2 shows the differential spectra from these experiments, which are very similar to those from the experiments with a single, higher Cl dosage. In particular, the peak near 270 nm appears even at the lowest Cl dosages investigated, supporting the idea that some key features of the reaction between NOM and Cl are identical from the very first attack of Cl on unaltered NOM to the attacks that occur after a substantial amount of Cl incorporation and chromophore alteration have taken place.

The differential spectra at very low Cl dosages also have some features that distinguish them from the corresponding spectra at higher dosages. Specifically, a small secondary peak is present in the spectrum near λ = 300 nm at low Cl dosages but not at larger dosages. This feature, which is indicative of some difference in the reaction of Cl with unaltered versus altered NOM molecules, may be a spectral manifestation of halogen attack on a well-defined, highly reactive functional group (according to current theories, most likely an aromatic β-diketone).[22]

Assuming that Cl attacks NOM predominantly at activated aromatic sites (aromatic sites substituted with oxygen-containing functional groups),[14,15,22,23] the band near 270 nm in the differential UV spectra must be generated by the selective destruction of these chromophores. According to Korshin et al,[13] the presence of a composite absorbance band (the ET band) centered near 255 nm is characteristic of unaltered NOM. This band is thought to be an indicator of the concentration of all aromatic functional groups (both activated and unactivated) in the sample. The maximum in the differential UV spectrum (which characterizes the selective loss of activated aromatic structures) is at longer wavelengths (265–270 nm) than the ET band of unaltered NOM (which characterizes all aromatic structures in unaltered NOM). This fact suggests that activated aromatic structures absorb light at longer wavelengths than do their unactivated counterparts.

Although the first attacks of Cl on NOM molecules might be at a narrowly defined group of reactive sites, as the reaction proceeds, the range of sites attacked presumably expands to include progressively less-reactive sites. The fact that the peak in the differential spectrum remains at the same wavelength throughout this process suggests that the basic structure of the reactive sites remains the same. Nevertheless, the expanding population of sites under attack is confirmed by a gradual increase in the width of the differential spectrum. This increase can be seen most easily when the differential spectra are normalized by dividing the absorbance at each wavelength by the maximum absorbance at any wavelength in the spectrum (ΔA^{max}), as shown in Eq 4:

$$\Delta A_{\lambda}^{normalized} = \frac{\Delta A_{\lambda}}{\Delta A^{max}} \qquad (4)$$

Such a normalization has the effect of assigning a value of 1.0 to the absorbance at the peak of the differential spectrum and representing absorbance at all other wavelengths relative to that value. The differential spectra in Figure 2 are replotted as normalized differential spectra in Figure 3; in this figure, the gradual widening of the differential spectra with increasing Cl dosage is apparent.

Figure 4 shows the UV spectra of raw and treated water from one of the French utilities. These spectra are typical of those from all the utilities investigated. Treatment decreases absorbance across the spectrum, especially at wavelengths between approximately 260 and 300 nm. As shown in Table 2, treatment always leads to a decrease in $SUVA_{254}$, suggesting that at these plants, treatment selectively removes or destroys NOM molecules enriched in aromatic chromophores.

As a result, the NOM remaining after treatment is likely to be considerably more hydrophilic than the NOM in the raw water. All of these changes indicate that although the NOM in the raw water and that remaining in solution after treatment obviously have overlapping characteristics, they do differ from one another in consistent and significant ways. Nevertheless, the differential spectra generated by chlorination of these water samples were extremely simi-

lar to each other and to those generated by chlorination of Judy Reservoir water. The differential spectra of water from utility 4 are typical of those from all sampling events at all the utilities (even those employing ozonation) and are shown in Figure 5.

Average differential spectra for a group of *n* samples from a given site can be calculated using Eq 5.

$$\Delta A_{\lambda}^{\text{average}} = \frac{\sum_{i}^{n} \Delta A_{\lambda}}{n} \qquad (5)$$

Like individual differential spectra, average differential spectra can be normalized by applying Eq 4. Figure 6 shows normalized average differential spectra for chlorination of three samples (taken on different dates) of raw and treated water from each utility along with a global average differential spectrum for all the samples. The similarity of these spectra is quite remarkable, considering the different water sources and treatment techniques applied prior to the chlorination step.

The maximum of the global spectrum in Figure 6 is at 266 nm, with an intensity approximately 33 percent greater than that at 254 nm. It is preferable to use ΔA at the higher wavelengths to follow the progress of the chlorination reaction because ΔA_{λ} is larger at $265 < \lambda < 275$ nm than at 254 nm and because, if residual Cl is quenched with Na_2SO_3, excess sulfite may contribute some absorbance at 254 nm and generate scatter in the data. Nevertheless, the reaction can be followed based on the absorbance at 254 nm, and the data collected by SAUR as part of this study are at that wavelength.

Differential UV spectra and DBP formation. ***Relationship of ΔA_{272} and TOX.*** Figure 7 shows the relationship between TOX formation and ΔA_{272} for chlorinated Judy Reservoir water and for two samples each of raw and treated water from all five French utilities. The relationship is linear and very strong ($R^2 = 0.99$) and is virtually identical to that reported previously[16] for other water samples and chlorination conditions. The figure shows the line derived from earlier experiments (all of which were conducted using low-bromide water), along with the best-fit line for the current experiments.

The TOX analysis yields information on the total molar concentration of organic halide in the sample, expressed as Cl. Thus, the value shown on the ordinate in Figure 7 includes contributions of both organic bromide (TOBr) and organic chloride (TOCl) species. The most direct way of interpreting the value is that the concentration shown (in micrograms per litre) divided by 35.5 gives the sum of TOBr and TOCl in micromoles per litre.

FIGURE 7 **Relationship of TOX to ΔA_{272} at varying Cl-to-DOC ratios, reaction times, and bromide concentrations**

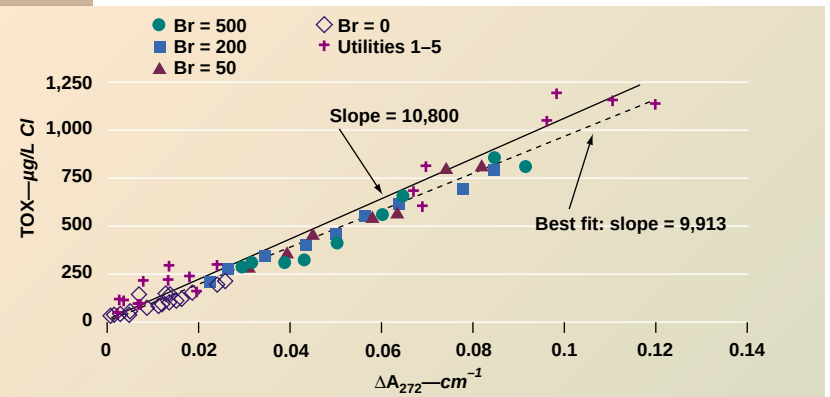

Open data points are for Judy Reservoir water, low Cl-to-DOC ratios (0.0029: 0.05 mg Cl_2/mg DOC), and 24–48-h reaction times. Filled data points are for Judy Reservoir water, a Cl-to-DOC ratio of 4 mg Cl_2/mg DOC, reaction times from 30 s to 24 h and bromide concentrations from 50 to 500 µg/L. Pluses are for French raw water samples. All data at pH 7.0. Solid line is the best fit for previous experiments reported elsewhere.[16]

The correspondence of the data from the current experiments for water samples containing up to 500 µg/L bromide with those reported earlier indicates that the relationship between TOX formation and ΔA_{272} is independent of bromide concentration, when TOX is expressed on a molar basis, i.e., µmol of organic halogen per litre. This result can be explained by the fact that ΔA_{272} detects and measures the disappearance of functional groups in NOM that form DBPs; it does not detect or measure the DBPs themselves. The fact that a single correlation fits the data for formation of both chlorinated and brominated DBPs supports the hypothesis that the organic precursors and the mechanism of the halogenation reaction are the same, regardless of which halogen is involved. Similarly, the fact that the data from the experiments with very low ratios of Cl to DOC fall on the line characterizing the higher Cl-to-DOC data reinforces the contention that Cl incorporation into NOM molecules occurs at similar sites and by similar pathways from the very beginning to the very end of the NOM–Cl reaction.

Figure 8 shows the efficiency of Cl incorporation into NOM as a function of Cl dosage in the system characterized in Figures 2 and 3. In these experiments, the Cl residual was nondetectable (<0.01 mg/L) in all cases, so Cl consumption can be equated with the Cl dosage. The curve for the cumulative incorporation indicates the ratio of TOX formed to the Cl dosage (comparing the conditions in each solution with the initial solution) whereas the curve for the differential incorporation indicates the same ratio for a running average of the three most recent Cl additions. That is, mathematically:

FIGURE 8 Cumulative and differential efficiency of Cl incorporation into NOM

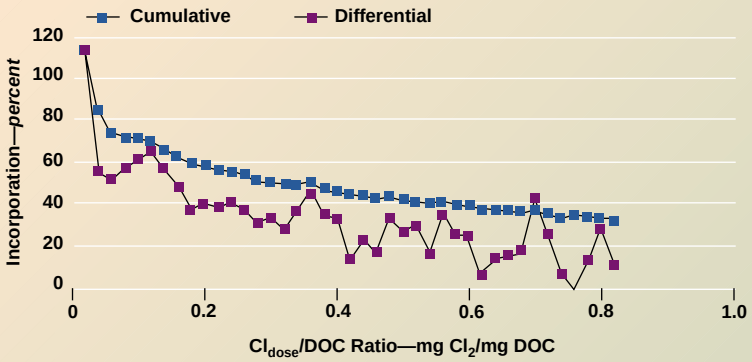

pH—7.0, DOC—5.2 mg/L, Cl dose—0.1 to 5.4 mg/L as Cl_2, reaction time—1 to 48 h

$$(\text{Cumulative percent incorporation})_i \equiv \frac{\text{TOX}_i}{(\text{Cumulative Cl consumption})_i} \quad (6)$$

$$(\text{Differential percent incorporation})_i \equiv \text{TOX}_i - \text{TOX}_{i-3}/[(\text{Cumulative Cl consumption})_i - (\text{Cumulative Cl Consumption})_{i-3}] \quad (7)$$

in which i indicates the number of Cl dosages that have been added to the solution.

At very low Cl dosages, almost 100 percent of the Cl was incorporated into NOM molecules. At later stages of the reaction, however, the efficiency of incorporation dropped to <10 percent, meaning that all the Cl added to the solution was consumed, but almost none of it became part of NOM molecules. Rather, the Cl must have oxidized unaltered or chlorinated NOM and been reduced to Cl^-.

This result provides key new information about the stoichiometry of NOM–Cl reactions, which will be useful for developing more realistic models of the reaction sequence. At the same time, it demonstrates the power of the TOX-versus-ΔA relationship; obtaining these data required only a small fraction of the time and effort that would have been required using conventional analyses.

Figure 9 demonstrates the use of the ΔA_{272}–TOX relationship to follow the kinetics of TOX formation. In this experiment, a well-mixed solution containing 4.4 mg/L DOC from Judy Reservoir was dosed with NaOCl (5.0 mg/L as Cl_2), after which it was pumped continuously through a flow cell in the spectrophotometer. The solution was dosed in-line with Na_2SO_3 at a point approximately one second upstream of the flow cell. The absorbance of the solution at 272 nm was monitored and was converted to TOX, based on the relationship shown in Figure 7. Because the hydraulic residence time in the flow cell was approximately 1 min, data at time <1 min are not reported. However, simple modifications of the experimental apparatus would allow reliable data to be collected much sooner (within a few seconds of mixing the NOM and Cl).

TOX formation in this experiment for 1 min < t < 1,000 min could be represented by the equation

$$\text{TOX} = 79 + 32 \log_{10}(t) \quad (R^2 = 0.099) \quad (8)$$

Although Eq 8 fits the experimental data very well, both the constants and the general form of the equation reflect the particular experimental conditions investigated and might not apply in other situations. For this reason, the details of Eq 8 are not considered especially significant. Rather, the importance of Figure 9 is that it demonstrates the immense amount of kinetic data for TOX formation that can be collected with very little effort when ΔA is used as a surrogate.

To develop a general kinetic expression for TOX formation, it would be necessary to carry out experiments like the one described earlier but estimating the concentrations of free Cl and reactive sites semicontinuously, along with that of TOX. The kinetics of Cl decay in the system could be analyzed relatively easily, perhaps using a spectrophotometric technique with a time resolution comparable to that for TOX.

On the other hand, estimating the concentration of reactive sites in unaltered NOM is a major challenge, let alone measuring the rate of change of this concentration during the chlorination reaction. No direct analytical technique exists for such measurements. Although the DOC concentration and A_{254} have been explored as potential surrogates for the concentration of precursor sites in NOM, they have not proved satisfactory. The inadequacy of these parameters is evident from the fact that DOC decreases negligibly and A_{254} can decrease by as little as 20 percent to as much as 95 percent during TOX formation potential (TOXFP) experiments, whereas TOX precursors are presumably almost completely destroyed.

One logical way of estimating the concentration of unreacted precursor sites [S] is as the difference between the maximum amount of TOX that could be formed by chlorination of the sample (the TOXFP) and the amount of TOX that has actually formed, i.e.,

$$[\text{S}] = \text{TOXFP} - \text{TOX}_t \quad (9)$$

Eq 9 can be expressed in terms of ΔA_{272} by substituting from Eq 2:

$$[S] = k\,(\Delta A_{272}^{TOXFP} - \Delta A_{272}^{t}) \quad (10)$$

in which ΔA_{272}^{t} is the instantaneous value of ΔA_{272} at any time t during a chlorination process and ΔA_{272}^{TOXFP} is the corresponding value under TOXFP conditions. Use of Eq 10 to estimate [S], ΔA_{272} to estimate TOX formation, and a spectrophotometric or amperometric technique to measure free Cl could allow researchers to develop an immensely richer data set than has previously been available for analyzing the kinetics of TOX formation. Such data sets are likely to yield important insights into the fundamental rate expression for the reaction.

FIGURE 9 Kinetics of TOX formation, based on semicontinuous monitoring of ΔA_{272}

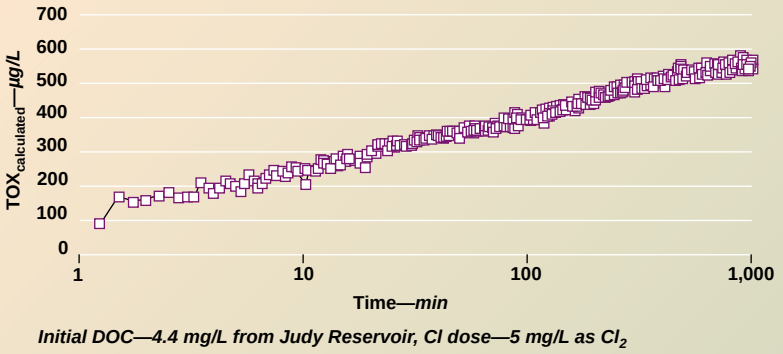

Initial DOC—4.4 mg/L from Judy Reservoir, Cl dose—5 mg/L as Cl_2

Relationship of ΔA_{272} to specific DBPs. The correlation shown in Figure 7 permits the total yield of halogenated by-products to be evaluated easily and rapidly in virtually any system of interest. However, for both regulatory compliance and an improved understanding of DBP formation in general, it is important to track the formation of individual DBP species as well. Therefore, the relationships between the formation of THMs and HAAs and the corresponding decrease in UV absorbance were explored.

Figure 10 shows the concentrations of specific DBPs as a function of ΔA_{272} in various experiments. For the French water samples, ΔA was measured only at 254 nm, so ΔA_{272} values are estimated based on the approximation derived from Figure 6 that $\Delta A_{272} = 1.33\ \Delta A_{254}$.

For each DBP, the data follow the pattern reported previously for the ΔA_{254}-versus-$CHCl_3$ relationship (Eq 3). That is, virtually none of these DBPs are formed at low values of ΔA_{272} (low TOX formation), but after some critical ΔA_{272} value has been exceeded, the concentration of each DBP increases substantially and approximately linearly with increasing ΔA_{272}. The equations of the best-fit lines through the data for total THMs, dichloroacetic acid (DCAA), and trichloroacetic acid (TCAA) in Figure 10 are

Judy Reservoir (Figure 10, part A):
THM = 2,481 (ΔA_{272} – 0.026)
DCAA = 1,364 (ΔA_{272} – 0.031)
TCAA = 3,132 (ΔA_{272} – 0.038)
French utilities (Figure 10, part B)
THM = 2,304 (ΔA_{272} – 0.011)

in which all the DBP concentrations are expressed in µg/L Cl (again including contributions from both brominated and chlorinated species) and ΔA_{272} is in cm^{-1}.

Bromide levels in these experiments ranged from below the detection limit of 25 µg/L (Judy Reservoir and utility 1) to 215 ± 77 µg/L (utility 5), and substantial concentrations of brominated THMs formed in some cases. In the extreme, when the treated water with the highest bromide concentration (utility 5) was chlorinated, bromine accounted for 53 mol percent of the halogen in the THMs formed. The absence of any discernible effect of bromide concentration on the relationship of ΔA_{272} to DBP, even in systems where brominated DBPs dominate over chlorinated ones, reinforces the conclusion drawn earlier that Br and Cl attack the same sites in NOM precursors via the same mechanism.

As noted earlier, the absence of the relatively small, polyhalogenated DBPs (THMs, DCAA, and TCAA) at low ΔA_{272} values can be attributed to the fact that some halogen is incorporated into sites distributed throughout NOM molecules from the instant that hypochlorite or hypobromite species begin reacting with NOM, but di- and trihalogenated DBPs are not released until later in the reaction, after two or three halogen atoms have clustered at a particular site.

According to this view of the reaction sequence, increasing the concentration of reactive NOM sites in the system should increase the amount of TOX that forms before polyhalogenated sites are created and compounds such as THMs are released, other factors being equal. In such a case, the value of ΔA^0 in Eq 3 would increase with increasing NOM concentration, causing plots of specific DBP concentration versus ΔA to have different x-intercepts for chlorination of water with different concentrations of reactive sites. However, the slope and intercept of this relationship also depend on pH[13] and perhaps other water quality variables. At this time, the data available are insufficient to test the dependence of ΔA^0 on NOM concentration.

Future research might identify approaches for predicting ΔA^0 values and the slopes of the lines relating $CHCl_3$, DCAA, and TCAA to ΔA_{272}. Even if no universal predictive equations are found, however, part

FIGURE 10 **$CHCl_3$ and HAA generation by chlorination of Judy Reservoir NOM (A) and total THM data for water from utilities 1-5 (B), as a function of ΔA_{272}**

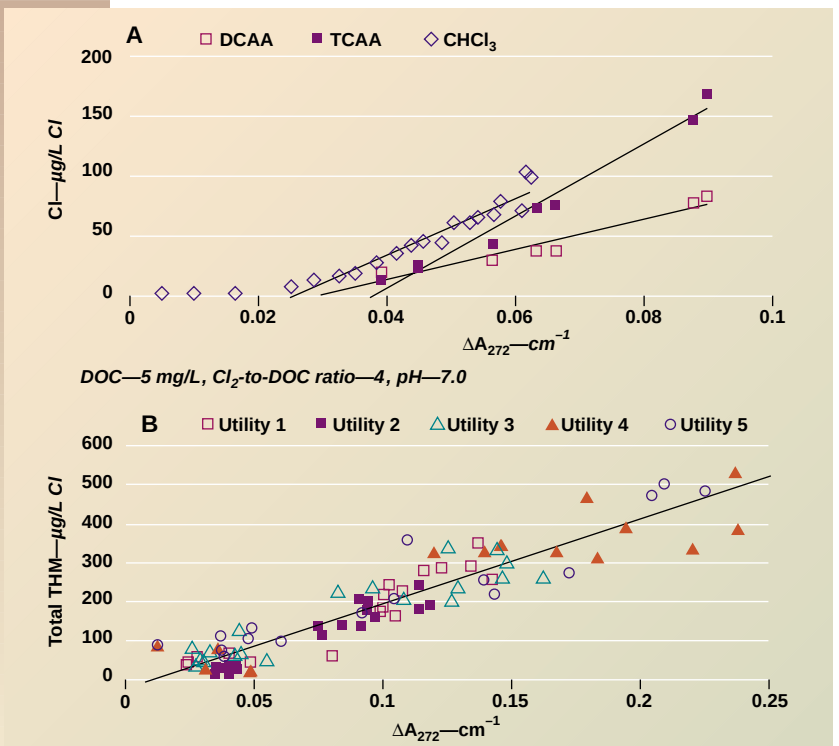

A of Figure 10 strongly supports the contention that under many circumstances, a simple and reliable equation could be established for these relationships for a given NOM source. ΔA_{272} could then be used as a surrogate for DBP formation at that site, applicable to the low concentrations of regulatory concern. In such a case, monitoring on a virtually continuous basis for these DBPs would be possible at a cost comparable to or even less than that currently required to conduct even a few analyses. Furthermore, the same instrumentation and analysis would simultaneously provide information about TOX formation and possibly the formation of other DBPs, pending the development and confirmation of relationships between ΔA_{272} and those species.

The preceding statements apply if formation of brominated DBPs is relatively unimportant in the particular water of interest. If brominated DBPs represent a significant fraction of the total DBPs, ΔA_{272} could still be used as a surrogate for DBP formation; however, it would be an indicator of total THMs, dihaloacetic acids, and trihaloacetic acids, rather than of just the chlorinated species. It is important to recognize that in such a case, the correlation would provide information about the molar concentration of halogenated compounds formed, not their mass. Maximum contaminant levels for DBPs are currently established as mass concentrations, so although the correlation would provide useful information about DBP formation, it would not be directly useful for monitoring for regulatory compliance. With additional research, correlations might be found to allow the speciation of the DBPs to be predicted based on ΔA, the bromide concentration, and other characteristics of the water. Such correlations could then be used in conjunction with ΔA to convert mole-based concentrations to mass-based concentrations.

The correlations described in the preceding paragraph help explain why the development of a universal correlation between spectral characteristics of unaltered NOM (e.g., A_{254}) and DBP formation potential (DBPFP) has been so difficult. Specifically, A_{254} might be a reasonable indicator of the aromatic content of NOM, as suggested by several researchers.[11,12] NOM contains both activated and unactivated aromatic groups, however, and it appears that the activated groups are the only ones (or at least the dominant ones) that participate in DBP-forming reactions. Thus, A_{254} measures a collection of functional groups, of which only a fraction are related to the parameter of interest (DBP formation).

If NOM from different sources contains different relative amounts of activated and unactivated aromatic groups, then no universal relationship between A_{254} and DBPFP would be expected. This hypothesis also highlights the utility of differential spectroscopy and explains why it is so successful as an indicator of DBP formation. In contrast to A_{254}, ΔA_{254} (or ΔA_{272}) measures only those functional groups that do participate in the NOM-Cl reaction. Furthermore, because ΔA_{λ} measures the extent to which the reaction has proceeded rather than the ultimate potential for it to proceed, this parameter can track DBP formation throughout the course of the reaction.

Use of the ΔA_{272}–DBP relationships in water treatment plants, distribution systems, and future research. Although use of the ΔA_{272}–TOX correlation for direct monitoring of DBPs throughout a distribution system is attractive in the abstract, it is probably unrealistic. Fluctuations in both the UV absorbance of treated water that is about to undergo chlorination and the residence time of water in the distribution sys-

tem effectively preclude accurate analysis of ΔA_{272} on the same batch of water at the plant outlet and a distant point in the distribution system.

The type of correlations described in this article, however, could be used to monitor DBP formation during a chlorine-contacting step in a plant or immediately downstream. Kinetic data such as those shown in Figure 9 could then be used to estimate what DBP concentration will be found at various downstream points in the system. The reliability of this approach (even in highly treated water) is supported by Figures 5 and 6, which demonstrate that ΔA can be measured consistently in such water, and part A of Figure 10, which demonstrates that the correlations apply even at very low values of ΔA and DBP formation. As noted earlier, the correlations can also be extremely useful for evaluating DBP formation in laboratory or pilot-scale treatability studies and for research into the mechanisms and kinetics of the DBP-forming reactions.

The fact that a single correlation fits the data for formation of both chlorinated and brominated DBPs supports the hypothesis that the organic precursors and the mechanism of the halogenation reaction are the same, regardless of which halogen is involved.

Accurate estimation of specific DBPs at low levels requires calibration of the equations with the water source of interest and use of a high-quality spectrophotometer in accord with a consistent protocol. If data are pooled from a variety of water sources or if the analytical protocol is not the same for all samples tested, the accuracy of the correlations will decline. For instance, part B of Figure 10 includes data from several water sources and for samples that contained varying amounts of free Cl (which was not quenched in these experiments). As a result, the data at low ΔA in the figure are qualitatively consistent with the data farther from the origin and with those collected under more rigorously controlled conditions, but they do not provide accurate estimates of the DBP concentrations in the samples.

Summary and conclusions

Chlorination of NOM causes its UV absorbance to decrease because of the alteration or destruction of aromatic chromophores. These changes can be characterized by the differential UV spectrum of the water. Differential UV spectra of chlorinated NOM are remarkably uniform for a wide range of water sources, water qualities, and chlorination conditions, exhibiting a moderately broad band with a maximum near a wavelength of 272 nm. This result reinforces the hypothesis that the nature of reaction sites susceptible to halogenation is extremely consistent in different water sources and throughout the period of reaction.

The magnitude of ΔA_{272} is an excellent indicator of TOX formation resulting from chlorination. The linear relationship between these two variables is independent of the Cl-to-DOC ratio, bromide concentration, pH from 5 to 11, reaction time, and NOM source. Although the values of several water quality parameters and the conditions of chlorination (e.g., time of reaction) affect the kinetics and ultimate amount of both TOX formation and chromophore destruction, the effects of each of these parameters on TOX and ΔA_{λ} are always proportional, so the relationship between the latter two parameters is unaffected.

A comparison of TOX formation (as inferred from ΔA_{272}) and Cl consumption indicates that the fate of Cl that reacts with NOM changes dramatically as the reaction proceeds. In the initial reactions between Cl and NOM, virtually 100 percent of the Cl that reacts is incorporated into the organic molecule. However, as the reaction proceeds (i.e., as reaction time or Cl dosage increases), less and less of the Cl that reacts is incorporated into the NOM molecules. Instead, most if not all of the Cl that reacts later in the process is reduced to Cl^- and is released to the solution. The ease with which this information was gathered illustrates the potential value of the ΔA–TOX relationship as a tool for advancing research into DBP-forming reactions. The specific information about variable Cl incorporation efficiency provides important new insights into the process of DBP formation.

The formation of THMs and individual HAAs is also well-correlated with ΔA_{272}, but unlike the TOX–ΔA_{272} relationship, the correlation is pH-dependent as reported previously[13,16] and cannot be represented by a straight line through the origin. For each sample, a range of ΔA_{272} values exists below which little or no THMs and HAAs are released. Further development of these relationships could dramatically reduce the cost of monitoring these DBPs (and perhaps others as well) and simultaneously allow performance of virtually instantaneous and continuous monitoring.

Acknowledgment

The authors thank Jerry Leenheer of the US Geo-

logical Survey, J.P. Croué of Université de Poitiers (France), and Yujung Chang of the University of Washington (Seattle) for their participation in valuable discussions of the concepts presented in the article. The authors acknowledge the financial support provided by the AWWA Research Foundation, HDR Engineering Inc. (Omaha, Neb.), Dynamco (West Sussex, England), and Societé d'Amenagement Urbain et Rurale (SAUR) (Maurepas, France). The authors also appreciate the assistance of Alain Deguin and Eric Lefebvre of SAUR in providing samples and analytical data.

References

1. MILLER, J.W. & UDEN, P.C. Characterization of Aqueous Chlorination Products of Humic Substances. *Envir. Sci. & Technol.*, 17:150 (1983).
2. KANNIGANTI, R. ET AL. Identification of Compounds in Mutagenic Extracts of Aqueous Monochloraminated Fulvic Acid. *Envir. Sci. & Technol.*, 26:1998 (1992).
3. CHRISTMAN, R.F. ET AL. Identity and Yield of Major Halogenated Products of Aquatic Fulvic Acid Chlorination. *Envir. Sci. & Technol.*, 17:625 (1983).
4. KRASNER, S.W ET AL. Occurrence of Disinfection By-products in US Drinking Water. *Jour. AWWA*, 81:8:41 (Aug. 1989).
5. James M. Montgomery Consulting Engineers. Mathematical Modeling of the Formation of THMs and HAAs in Chlorinated Natural Waters. (IP-5C-55010-9/93-CM) AWWARF, Denver (1993).
6. HARRINGTON, G.W.; CHOWDHURY, Z.K.; & OWEN, D.M. Developing a Computer Model to Simulate DBP Formation During Water Treatment. *Jour. AWWA*, 84:11:78 (Nov. 1992).
7. RATHBUN, R.E. Regression Equations for Disinfection By-Products for the Mississippi, Ohio, and Missouri Rivers. *Sci. Total Envir.*, 191:235 (1996).
8. GARCIA-VILLANOVA, R.J. ET AL. Formation, Evolution, and Modeling of Trihalomethanes in the Drinking Water of a Town. I. At the Municipal Treatment Utilities. *Water Res.*, 31:1299 (1997).
9. JAFFE, H.H & ORCHIN, M. *Theory and Applications of Ultraviolet Spectroscopy*. John Wiley & Sons, New York (1962).
10. SCOTT, A.I. *Interpretation of the Ultraviolet Spectra of Natural Products*. Pergamon Press, New York (1964).
11. TRAINA, S.J.; NOVAK, J.; & SMECK, N.E. An Ultraviolet Absorbance Method of Estimating the Percent Aromatic Carbon Content in Humic Acids. *Jour. Envir. Qual.*, 19:151 (1990).
12. NOVAK, J.; MILLS, G.L.; & BERTSCH, P.M. Estimating the Percent Aromatic Carbon in Soil and Aquatic Humic Substances Using Ultraviolet Absorbance Spectroscopy. *Jour. Envir. Qual.*, 21:144 (1992).
13. KORSHIN G.V.; LI, C-W.; & BENJAMIN, M.M. Use of UV Spectroscopy to Study Chlorination of Natural Organic Matter. *Disinfection By-Products and NOM Precursors: Chemistry, Characterization, Control* (R. Minear and G. Amy, editors). ACS, Washington (1996).
14. ROOK, J.J. Chlorination Reactions of Fulvic Acids in Natural Waters. *Envir. Sci. & Technol.*, 11:478 (1977).
15. BOYCE, S.D. & HORNIG, J.F. Reaction Pathways of Trihalomethane Formation From the Halogenation of Dihydroxyaromatic Model Compounds for Humic Acid. *Envir. Sci. & Technol.*, 17:202 (1983).
16. KORSHIN G.V.; LI, C-W.; & BENJAMIN, M.M. Decrease of UV Absorbance as an Indicator of TOX Formation. *Water Res.*, 31:4:946 (1997).
17. STEVENS, A.A.; MOORE, L.A.; & MILTNER, R.J. Formation and Control of Non-trihalomethane Disinfection By-products. *Jour. AWWA*, 81:11:54 (Nov. 1989).
18. CHANG, Y-J.; LI, C-W.; & BENJAMIN, M.M. Use of Iron Oxide–coated Media for NOM Sorption and Particulate Filtration. *Jour. AWWA*, 89:5:100 (May 1997).
19. *Standard Methods for the Examination of Water and Wastewater*. APHA, AWWA, and WEF, Washington (19th ed., 1995).
20. HODGE, J.W. & BECKER, D. Determination of Haloacetic Acids and Dalapon in Drinking Water by Ion-Exchange Liquid–Solid Extraction and Gas Chromatography With an Electron Capture Detector. USEPA Method 552.1 (1992).
21. AFNOR T 90-125. Dosage des Hydrocarbures Halogénés Hautement Volatils. Méthodes par Chromatographie en Phase Gazeuse. *Qualité de l'Eau*. (1997).
22. LARSON, R.A. & WEBER, E.J. *Reaction Mechanisms in Environmental Organic Chemistry*. Lewis Publishers, Boca Raton, Fla. (1994).
23. TRETYAKOVA, N.Y.; LEBEDEV, A.T.; & PETROSYAN, V.S. Degradative Pathways for Aqueous Chlorination of Orcinol. *Envir. Sci. & Technol.*, 28:606 (1994).
24. EDZWALD, J.K.; BECKER, W.C.; & WATTIER, K.L. Surrogate Parameters for Monitoring Organic Matter and THM Precursors. *Jour. AWWA*, 77:4:122 (Apr. 1985).

About the authors: *Chi-Wang Li is a research associate in the Department of Civil Engineering, Box 352700, University of Washington, Seattle, WA 98195-2700. He has a BS degree from Tam Kang University, Taipei, Taiwan, and MSE and PhD degrees from the University of Washington in Seattle. Gregory V. Korshin is a research assistant professor, and Mark M. Benjamin is a professor, both at the University of Washington in the Department of Civil Engineering.*